J Biomol NMR (2009) 45:319–327
DOI 10.1007/s10858-009-9374-3

ARTICLE

Characterization of different water pools in solid-state NMR protein samples

Anja Böckmann · Carole Gardiennet · René Verel · Andreas Hunkeler · Antoine Loquet · Guido Pintacuda · Lyndon Emsley · Beat H. Meier · Anne Lesage

Received: 22 July 2009 / Accepted: 4 September 2009 / Published online: 25 September 2009

Abstract We observed and characterized two distinct signals originating from different pools of water protons in solid-state NMR protein samples, namely from crystal water which exchanges polarization with the protein (on the NMR timescale) and is located in the protein-rich fraction at the periphery of the magic-angle spinning (MAS) sample container, and supernatant water located close to the axis of the sample container. The polarization transfer between the water and the protein can be probed by two-dimensional exchange spectroscopy, and we show that the supernatant water does not interact with protein on the timescale of the experiments. The two water pools have different spectroscopic properties, including resonance frequency, longitudinal, transverse and rotating frame relaxation times. The supernatant water can be removed almost completely physically or can be frozen selectively. Both measures lead to an enhancement of the quality factor of the probe circuit, accompanied by an improvement of the experimental signal/noise, and greatly simplify solvent-suppression by substantially reducing the water signal. We also present a tool, which allows filling solid-state NMR sample containers in a more efficient manner, greatly reducing the amount of supernatant water and maximizing signal/noise.

Keywords Solid-state NMR · Water–protein polarization transfer · Microcrystalline protein · Chemical exchange

Electronic supplementary material The online version of this article (doi:10.1007/s10858-009-9374-3) contains supplementary material, which is available to authorized users.

A. Böckmann (✉) · C. Gardiennet · A. Loquet
Institut de Biologie et Chimie des Protéines, Université de Lyon, UMR 5086 CNRS/UCB-Lyon 1, 7 passage du Vercors, 69367 Lyon, France
e-mail: a.bockmann@ibcp.fr

R. Verel · A. Hunkeler · B. H. Meier
Physical Chemistry, ETH Zürich, Wolfgang-Pauli-Strasse 10, 8093 Zurich, Switzerland

G. Pintacuda · L. Emsley · A. Lesage
Université de Lyon, CNRS/ENS Lyon/UCB-Lyon 1, Centre RMN à Très Hauts Champs, 5 rue de la Doua, 69100 Villeurbanne, France

Introduction

High-resolution solid-state NMR spectroscopy using magic-angle spinning (MAS) has emerged over the last few years as a key technique for the structural investigation of solid biological samples (McDermott 2004; Tycko 2004; Baldus 2006; Böckmann 2007). In particular, it has been demonstrated that both three-dimensional (3D) structure (Castellani et al. 2002; Jaroniec et al. 2004; Lange et al. 2005; Zhou et al. 2007b; Loquet et al. 2008; Manolikas et al. 2008) and dynamics (Hologne et al. 2005; Giraud et al. 2005; Chevelkov et al. 2007, 2008; Lorieau and McDermott 2006; Ravindranathan et al. 2007) of insoluble proteins could be probed by NMR at an atomic resolution and in a site-specific way. Solid-state NMR spectroscopy has notably been successfully applied to large immobilized biological assemblies, like membrane-embedded proteins (Etzkorn et al. 2007; Schneider et al. 2008), fibrillar aggregates (Iwata et al. 2006; Wasmer et al. 2008), or intact virus proteins (Lorieau et al. 2008).

Because the biological function of such solid assemblies critically depends on their interactions with the solvent, and is generally characterized in the presence of it, the characterization of the polarization flow over the water–protein interface in solid biological matter is of great

interest. In this context, and in complement to related studies in solution NMR (Otting 1997; Modig et al. 2004; Halle 2003), our group and others have recently investigated the polarization transfer over the water–protein interface in solid proteins (Lesage and Böckmann 2003; Paulson et al. 2003; Böckmann et al. 2005; Chevelkov et al. 2005; Lesage et al. 2006; 2008, Zhou and Rienstra 2008). Polarization transfer between water and protein was found to be a subtle and complex process, which depends on interplaying pathways caused by different types of interactions between the protein and the solvent. In microcrystalline model proteins, pathways driven by chemical exchange, spin diffusion and cross relaxation have been characterized. Notably, fast chemical exchange was observed to be a major polarization-transfer mechanism between exchangeable protein protons (mainly on the sidechains) and solvent protons, as revealed through positive cross-peaks at the water frequency in two-dimensional (2D) heteronuclear correlation spectra. While chemical exchange, followed by spin diffusion, has been shown to be the dominant mechanism of interaction at room temperature (Lesage et al. 2008), we have recently demonstrated that at low temperatures, or at high MAS frequencies, the contribution from chemical exchange to the polarization of the chemically non-exchangeable protons of the proteins is reduced and ROE-like rotating frame polarization transfer from the solvent can become a significant source of water–protein polarization transfer, as revealed by negative signals at the water resonance.

In protein solutions at room temperature, all of the water is usually in interaction with the protein on the timescale of the NMR experiment. Fast chemical exchange leads to a single line for the protein exchangeable-proton resonances and the water resonance at an average position which, due to the higher abundance of water, is very close to the resonance position for pure water. The resulting water resonance is usually very narrow ($\sim$10 Hz FWHH). The observation of an equally narrow line in the solid-state spectra has led to the development of water-edited NMR experiments, based on relaxation filters, to probe the interface between solvent and membrane-bound proteins (Ader et al. 2009), as well as fibrils (Kumashiro et al. 1998; Etzkorn et al. 2007; Andronesi et al. 2008).

In this contribution, we show that there are actually two distinct pools of water molecules which can be observed and identified in the proton NMR spectra of proteins, and characterized according to their location in the sample container (rotor). A detailed characterization is performed for a microcrystalline sample of the Crh protein (Böckmann et al. 2003; Lesage and Böckmann 2003), and similar observations are shown for other proteins. The two resonances observed for water are assigned on one hand to water mainly located in the center of the rotor, here referred to as supernatant water, and on the other hand to the water in the crystallite-rich fraction, located either inside the channels of each crystallite or directly surrounding them (here referred to as crystal water). Two distinct water signals have also been observed for cell suspensions, and have been assigned to intracellular/interstitial water and cell-free (supernatant) water (Aime et al. 2005). The two water pools in our microcrystalline Crh sample are schematically represented in Fig. 1a. A typical one-dimensional (1D) proton spectrum observed for Crh is represented in Fig. 1b, showing two clearly distinct resonances, with different line widths and chemical shifts.

We show in the following that the narrow line in the spectrum belongs to the supernatant water, whereas the broader line ($\sim$60 Hz) is due to water in interaction with the protein. We demonstrate that the supernatant water does not interact with the protein on the timescale of our experiments, and, as it concentrates notably in the middle of the NMR rotor upon sample spinning, can be physically removed from the sample to a large extent. Also, we show that sample cooling can be used in favorable cases to freeze the supernatant water selectively and remove its resonance by broadening it beyond detection in a high-resolution setup, while NMR correlations are still observed between the protein residues and the second water pool, assigned to crystal

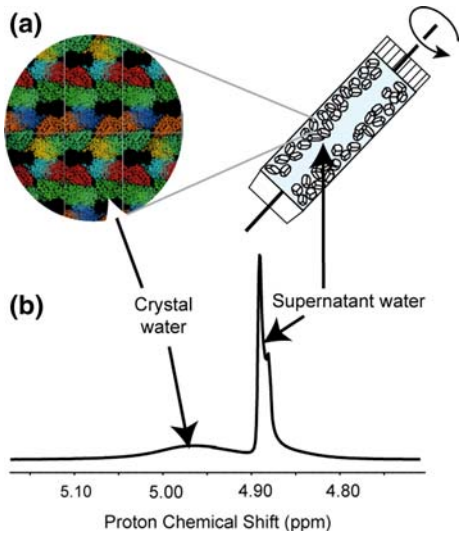

Fig. 1 **a** Schematic representation of protein microcrystals in the NMR rotor during sample spinning, together with a view of the crystal lattice of Crh. The center of the rotor is filled by supernatant water, while crystal water is present at the surface and in the channels of each crystallite. **b** Water proton NMR signals. The spectrum was recorded on an unlabeled sample of microcrystalline Crh, at 500 MHz, with a spinning frequency of 11 kHz and a sample temperature of about 12°C. At this temperature, two distinct resonances are observed, which are assigned to the supernatant and crystal-water pools (see the main text). The complex lineshape of the upfield resonance is likely due to thermal and/or magnetic field gradients

water. We show that removing the supernatant water may be useful in a variety of circumstances, from refilling the empty space in the rotor with protein to gain signal/noise, to improving the quality factor of the probe circuit with an associated gain in signal/noise and reduction in sample heating through radio-frequency power deposition, to enabling the use of direct proton-detection schemes without the need of water suppression in solid-state NMR of proteins.

Materials and methods

Sample preparation

Crh was overexpressed as described previously (Galinier et al. 1997) by growing bacteria in >98% ^{2}H, ^{13}C, ^{15}N labeled medium (S9, Martek). Exchangeable protons were back exchanged under denaturing conditions (6 M Guanidinium Chloride) and the protein was diluted sixfold for refolding into 20 mM NH_4HCO_3 and washed three times with 15 ml 20 mM NH_4HCO_3. The final protein concentration was 20 mg/ml. The protein was crystallized using 20% PEG 6000 in 20 mM NH_4HCO_3 as precipitant, in 300 µl drops in a nine well glass crystallization plate over 20 ml of 2 M NaCl solution (Böckmann et al. 2003). Equal volumes of protein solution and crystallization solution were used, resulting in a final PEG concentration of 10%. The crystallization solution comprising the protein was at pH 7. Crystals were harvested as soon as they appeared. The rotor was filled with microcrystals resulting from about 8 mg of protein.

NMR spectroscopy

NMR experiments were performed on a Bruker Avance III 500 MHz (proton frequency) spectrometer, equipped with a 4 mm double-resonance CPMAS probe for Figs. 1 and 2, on a Bruker Avance III 850 MHz spectrometer, equipped with a 1.3 mm double resonance CPMAS probe for Figs. 3 and 4, and on a Bruker Avance II 700 MHz spectrometer, equipped with a 3.2 mm triple resonance CPMAS probe for Figs. 5 and 6. Other experimental details are given in the figure captions. The chemical shift of the supernatant-water resonance was used to determine the sample temperature above the freezing point. Internal referencing to DSS providing the zero chemical shift, the temperature was determined using the relationship $\delta(H_20) = 7.83 - T/96.9$ ppm, with the temperature measured in Kelvin (Cavanagh et al. 1996). Below the freezing point of the supernatant water, the actual temperature was estimated from the reading of the sample temperature by the probe thermocouple, corrected by the difference observed between the measured and real temperature above the freezing point.

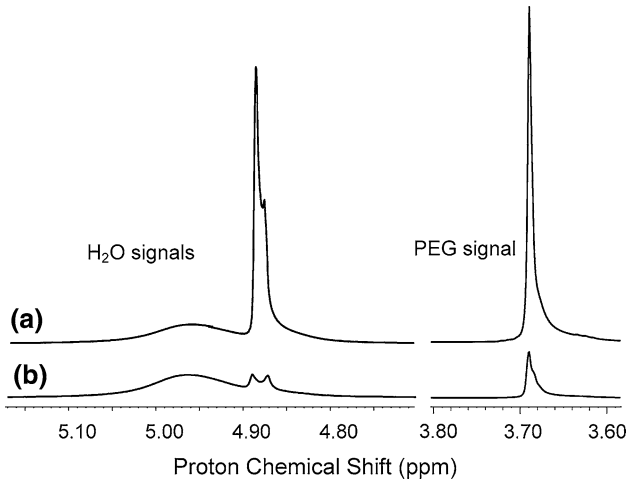

Fig. 2 One-dimensional proton spectra of water and PEG in microcrystalline Crh before (**a**) and after (**b**) pipetting out the supernatant water from the middle of the NMR rotor. The spectra were recorded at a proton frequency of 500 MHz, on a Bruker Avance III spectrometer, equipped with a 4 mm double resonance CPMAS probe, at a spinning frequency of 11 kHz and a sample temperature of 12°C. Spectrum (**b**) was recorded after pipetting about 50 µl of solvent from the rotor. The complex shape of the supernatant-water line at 4.87 ppm is attributed to thermal and/or magnetic field gradients over the sample

Results and discussion

Evidence for supernatant and crystal water

Figure 2a and b shows the 1D ^{1}H NMR spectrum of a sample of microcrystalline Crh recorded at a sample temperature of 12°C. At this temperature, three distinct resonances are observed: the PEG (polyethylene glycol) resonance at 3.74 ppm, and *two* water resonances: a narrow (6 Hz) and intense resonance at around 4.87 ppm, and a broader resonance (50 Hz) at 4.96 ppm of much lower peak height. These two water resonances can be unambiguously assigned to the two different water pools described above, namely the supernatant water for the resonance at 4.87 ppm, and the crystal water for the resonance at 4.96 ppm.

This assignment is based on a series of NMR experiments, as described below. The first consists simply in physically removing the supernatant water from the rotor. Indeed, upon sample spinning, the rotor acts as a centrifuge (11 kHz rotation in a 4 mm rotor (with a 2.6 mm inner diameter) corresponds to an acceleration at the wall of $633{,}000 \times g$) and the solvent concentrates in the center of the NMR rotor while the crystallites are centrifuged towards the rotor walls. By carefully pipetting out the solution located in the middle of the rotor after several hours of sample spinning, we observe that the resonance assigned to the supernatant water strongly decreases in peak height (spectrum in Fig. 2b), while that assigned to

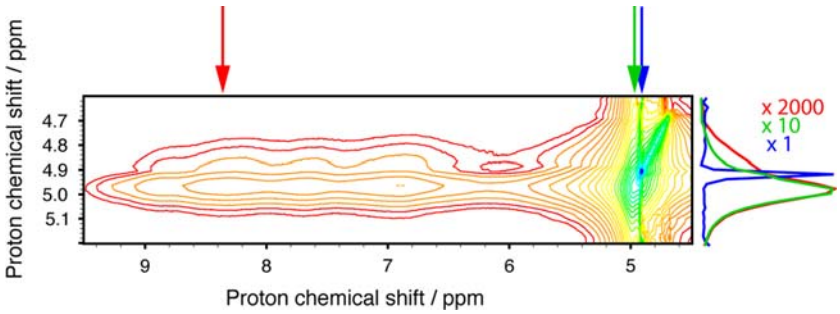

Fig. 3 Extract of a 2D EXSY spectrum recorded on deuterated microcrystalline Crh, at a MAS frequency of 55 kHz and with a longitudinal mixing time of 100 ms. Traces are shown at the right for different ω_2 frequencies: the supernatant-water signal (*blue*), the crystal-water signal (*green*), and the protein–water cross signals (*red*). A total of 4,096 t_1 increments with eight scans each were recorded with a recycle delay of 1 s (for a total experimental time of 9 h). The spectrum was recorded on an 850 MHz Bruker Avance III spectrometer equipped with a 1.3 mm CPMAS probe. The sample temperature was 10°C

the crystal water remains. About 80% of the initial content of supernatant water could be removed in this way, corresponding to about 50 µl (for a total rotor volume of 100 µl). Note that the height of the PEG resonance decreases in a similar way. The ^{13}C CP spectrum, as well as traces at the water frequency of a HETCOR spectrum, are shown in Supporting figure S1. In solution-state NMR, the large water signal is routinely suppressed by specialized pulse sequences that have recently been adapted for use in solids (Paulson et al. 2003; Zhou et al. 2007a; Zhou and Rienstra 2008). The physical removal of most of the water from the sample greatly simplifies these techniques or makes them unnecessary. This is expected to be notably a great advantage for samples containing additives like PEG or MPD (2-methylpentane-2,4-diol), or buffers like Tris, which require the simultaneous suppression of several resonances, or the use of expensive deuterated chemicals. We observed the above described distinct water resonances also in other protein samples studied in our laboratories, as shown in Supporting figure S2 for the examples of Ubiquitin and C4bp microcrystals, HET-s(218-289) fibrils, as well as the membrane anchor of Hepatitis C virus NS5A protein in liposomes.

A two-dimensional proton-EXSY (Exchange Spectroscopy) (Jeener et al. 1979; Meier and Ernst 1979) experiment with a longitudinal mixing time of 100 ms under fast MAS conditions confirms the assignment proposed for the two water signals. The experiment was carried out on a deuterated sample of microcrystalline Crh (Lesage and Böckmann 2003) crystallized in H_2O. Figure 3 shows an extract of the 2D spectrum around the water frequency in ω_1, and the water and resonances in the amide region in ω_2. Traces along ω_1 extracted at different ω_2 frequencies are shown: in blue, the trace at the supernatant-water frequency; in green, the trace at the crystal-water frequency; and in red the trace in the amide proton region. Clearly, cross-peaks are observed between the ω_1 frequency of the broad crystal-water signal and the protein protons. This polarization transfer can notably arise from chemical exchange combined with spin diffusion (Lesage et al. 2006, 2008; Böckmann et al. 2005; Lesage and Böckmann 2003). The narrow water resonance, on the contrary, does not give rise to detectable polarization transfer to the protein spins. The observed correlations confirm the assignment of the two water resonances: the narrow upfield water resonance corresponds to the supernatant water, while the broader resonance is assigned to the crystal water. This is consistent with previously observed chemical exchange-mediated correlations in 2D HETCOR spectra of deuterated Crh, for which linewidths of about 120 Hz were reported for water in the 2D maps (Böckmann et al. 2005).

No significant cross-peaks between the two water resonances were observed in EXSY spectra recorded with longitudinal mixing times ranging up to as long as 1 s (which is the effective detection limit imposed by the relaxation times in this system), indicating that the two water pools do not exchange on the time scale of the proton T_1s (data not shown), and thus do form two distinct and well separated solvent pools from the NMR point of view. The minimal physical separation of the two pools can thus, based on the self-diffusion coefficient of water (1.11×10^{-9} m^2 s^{-1} at 0°C) be estimated to 50 µm.

As shown in Fig. 4, relaxation measurements performed at 850 MHz indicate that the T_1 relaxation time of the narrow supernatant-water line is different from that of the broader crystal-water line. At a sample temperature of about 5°C, T_1 values of 0.99 and 0.60 s respectively were measured (the T_1 of protons in the amide proton region being of the order of 0.75 s). Under these experimental conditions, the full line width at half height (FWHH) of the crystal water was found to be about 90 Hz, compared to about 6 Hz for the supernatant-water line. The corresponding homogeneous line widths, evaluated from transverse relaxation time measurements according to

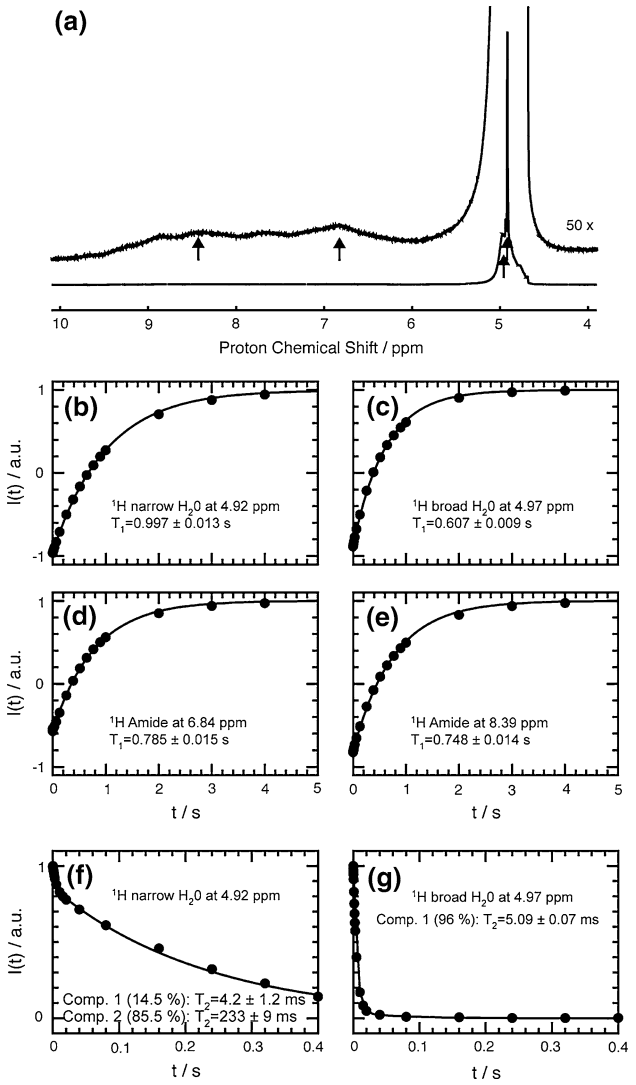

Fig. 4 Proton T_1 and T_2 (or T_2') measurements for the different resonances observed in a proton spectrum in a one-pulse ^1H experiment. The spectra were measured on a Bruker Avance III 850 MHz spectrometer, using a 1.3 mm CPMAS probe. A MAS rate of 55.5 kHz was used. **a** Spectrum of the deuterated Crh protein showing the two water resonances, as well as resonances in the amide proton region. **b** Data points measured in inversion-recovery experiments for the supernatant-water line; **c** for the crystal-water line; **d** for the amide signal at 6.84 ppm; and **e** for a frequency of 8.39 ppm. **f** Hahn-echo decays measured for the narrow component of the water line (supernatant water) and **g** for the broad component of the water line (crystal water)

$\Delta(\text{FWHH}) = 1/(\pi T_2)$ are 62 ± 1 Hz and 1.3 ± 0.1 Hz, respectively. This indicates that the supernatant-water line is heterogeneously broadened by imperfect shim and susceptibility or temperature differences while the broadening of the crystal-water resonance has a strong homogeneous component, possibly originating from chemical exchange with the labile protein amine and hydroxyl protons located downfield from the water frequency (vide infra). Note that the relatively short T_2 relaxation time of the crystal-water resonance (5 ms) may well explain why, in previous studies, T_2-filters designed to select the water frequency had to be chosen relatively short to enable the selection of water in interaction with the protein (Harbison et al. 1988; Böckmann et al. 2005; Andronesi et al. 2008). Transverse relaxation times show similar behavior, as shown in Supporting figure S3. $T_{1\rho}$ of the supernatant water can be determined to 375 ± 140 ms, in contrast to the crystal water with $T_{1\rho} = 11.1 \pm 0.5$ ms. The transverse relaxation curves measured for the signals in the amide proton region show multiple components, with $T_{1\rho} < 14$ ms.

Freezing out the supernatant water

At temperatures below −20°C, the supernatant water freezes and its resonance is broadened beyond detection in our setup, while the resonance from the crystal water can still be observed. This is illustrated in Fig. 5, which shows the evolution of the PEG and water proton resonances for a

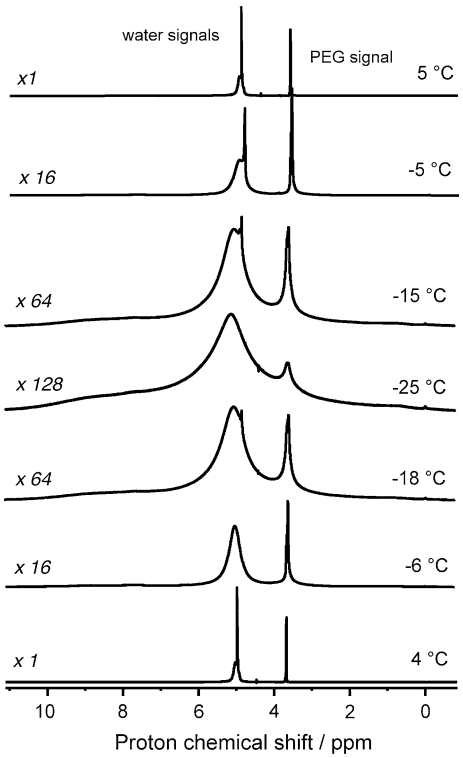

Fig. 5 One-dimensional proton spectra of deuterated microcrystalline Crh, as a function of temperature. These spectra were acquired after pipetting most of the supernatant water from the center of the NMR rotor (see main text). The sample temperature was derived from the residual supernatant-water chemical shift above the freezing point, and then extrapolated from the reading of the sample temperature by the probe thermocouple (see Materials and methods section). The two water resonances are observed at around 5 ppm, while the PEG and the amide protons resonate respectively at 3.7 and around 8 ppm. The spinning frequency was 9 kHz. The spectra were recorded at 700 MHz on a Bruker Avance II spectrometer

sample temperature ranging from 5 to −25°C. The line width of the crystal water gradually increases with decreasing temperatures, from about 100 Hz at 5°C to 1,000 Hz at −25°C. As shown in the figure, this broadening process, as well as the freezing of the supernatant water, is reversible with temperature.

In a crystal of Crh, 67% of the space is occupied by water [PDB code 1mu4 (Juy et al. 2003)] This means that there are ten times as many water protons (in fact at least 10 times because there is a certain amount of water outside the crystals that contributes to the crystal-water pool) in the crystal than amide and exchangeable sidechain protons from the protein, which is roughly in accordance with the integrals measured for the amide region and water signals in the spectrum recorded at −25°C shown in Fig. 5. Thus, at these temperatures, only the water within the crystallites may still be mobile. Interestingly, we note that upon freezing of the supernatant-water pool, the quality factor of the probe circuit is enhanced on the proton channel (due to lower electrical conductivity of the central part of the sample), and that a recalibration of the proton RF field is required. Differences in RF-power attenuation as large as 3 dB were found before and after freezing of the supernatant water (on a Bruker standard solenoid 4 mm double resonance CPMAS probe at 700 MHz proton frequency). A similar effect was observed after pipetting out a large fraction of the supernatant water from the rotor.

The evolution of the supernatant-water resonance as a function of temperature has been investigated in detail in reference (Lesage et al. 2008). The experiments described there were done on a similar sample, but containing a larger fraction of supernatant water and for which the crystal-water line could not be observed above the freezing point of the supernatant water. The resonance frequency of the supernatant-water signal has been shown to be mainly governed by the sample temperature and can indeed be used as a convenient thermometer for determining the real temperature inside the rotor (Gottlieb et al. 1997, Cavanagh et al. 1996). The behavior of the resonance of the crystal water, and notably its broadening, as a function of temperature, is more complex. This water is in fast chemical exchange with protein sidechain protons (hydroxyl and amine protons). It is therefore tempting to assume that the downfield shift of the crystal-water resonance, and the significant broadening, are a consequence of chemical exchange with sidechain protons that would resonate downfield from water in the range between about 5 ppm (Thr Hγ1) and 10 ppm (Tyr Hη).

A simplified model calculation for an asymmetric two-site exchange between resonances at 4.87 ppm (bulk water) and 9 ppm (as a rough estimation for fast exchanging side chain protons, e.g. His Hδ1, Hε2, Lys Hζ, Tyr Hη) with homogeneous linewidths of 1.3 and 125 Hz leads to a good prediction of the observed linewidth and position using a population ratio of water protons to exchangeable sidechain protons of 20:1 for an exchange rate constant of 2 to 4×10^5 s^{-1} (see Supporting figure S4). This value is in the range expected for the faster exchanging sidechains: lysine Hζ exchange with rate constants with up to 1.5×10^4 s^{-1} (for ubiquitin in liquid phase, at 290 K and pH 7.45 (Segawa et al. 2008) while histidine Hδ1/Hε2 exchange rates are, under these conditions, $>10^6$ s^{-1}, P. Pelupessy, personal communication). While the actual multisite exchange is much more complex than our model, the extent of observed homogeneous broadening and the resonance position of the crystal-water line are clearly explainable by chemical-exchange effects with labile sidechain protons. Further sources of line broadening for the crystal water like restricted mobility of the water molecules inside the microcrystals and the dipolar interaction between water protons and the protein protons cannot be excluded but the observed effects can be explained by chemical exchange only.

That no freezing of the water with the broad resonance peak was observed over the temperature range studied might be due to the fact that this water pool corresponds mainly to the water inside the crystal. Indeed, it is well known that the freezing point of water decreases proportionally to the radius of a capillary. This property, called the capillary effect, has been exploited in solution NMR where protein solutions in glass capillaries are used to investigate biomolecules in supercooled water (Skalicky et al. 2000, 2001), with sample temperature as low as −18°C. In this case the capillaries are formed by the spaces within the crystallites (Juy et al. 2003). Nanoconfined water can remain liquid down to 220 K (Mallamace et al. 2008).

Water–protein polarization transfer is still observed at −30°C

Figure 6a shows a directly detected proton spectrum obtained with a sample temperature of −30°C. Figure 6b shows the corresponding 1D carbon-13 filtered spectrum, where the proton polarization has been first transferred to the nearby carbon-13 nuclei by a CP step, before being back-transferred to the proton spins during a second CP period. This experiment was introduced by Zilm and coworkers to investigate polarization exchange among amide protons (Paulson et al. 2003). They showed that this experiment leads to the observation of correlations between amide and water protons in microcrystalline proteins. In the low temperature conditions we consider here, no water suppression scheme is required for direct proton acquisition since the vast majority of the solvent is broadened beyond detection. As shown in Fig. 6b, the water signal is fully eliminated in the ^{13}C-filtered experiment. However, when a

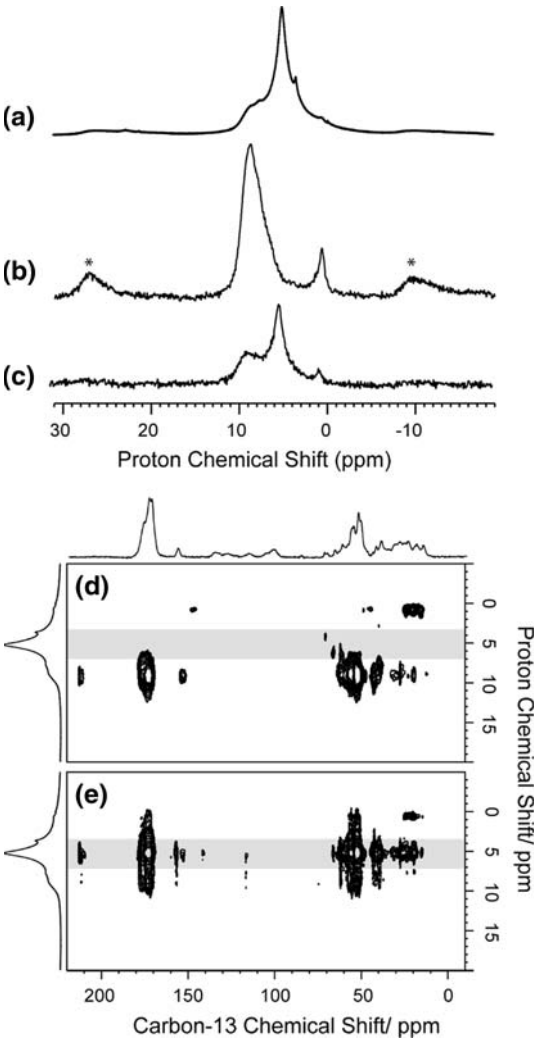

Fig. 6 **a** One-dimensional single-pulse proton spectrum of deuterated microcrystalline Crh recorded at a sample temperature of −30°C. Spectra were acquired after pipetting the supernatant water from the center of the NMR rotor (see main text). **b** One-dimensional ^{13}C-filtered proton spectrum (16 scans). The asterisks indicate spinning sidebands. **c** One-dimensional carbon-13 filtered proton spectrum in which a longitudinal mixing period of 25 ms has been added before detection (eight scans). Two-dimensional proton detected HETCOR spectrum. A total of 640 t_1 increments with eight scans each were recorded, with total acquisition times of 7.1 and 6.9 ms in t_1 and t_2, respectively. **e** A similar HETCOR spectrum acquired with the same acquisition parameters, but with an additional longitudinal mixing period of 15 ms before direct detection. For spectra of **b**–**e**, contact times of 1 and 2 ms were used for the two CP steps. The recycle delay was 2 s and the spinning frequency was 9 kHz. One-dimensional proton and carbon spectra are shown respectively to the left and above the 2D spectra. The spectra were recorded on a 700 MHz Bruker Avance II spectrometer, using a MAS triple resonance 3.2 mm probe. The water frequency is indicated in *grey*

longitudinal spin-exchange period is inserted after the second CP step, we observe polarization transfer from the protons in the amide region and methyl protons to the water protons, with a maximum transfer at a mixing time of about 25 ms (Fig. 6c). We recorded two-dimensional versions of these experiments in order to investigate more closely the polarization transfer between the protein and the water.

Figure 6d shows a 2D (^{1}H, ^{13}C) heteronuclear (HETCOR) correlation experiment, in which the proton polarization is transferred to the ^{13}C spins which evolve according to their chemical shift, before back polarizing to the proton nuclei for detection. No correlation is observed at the water frequency, indicating that no carbon polarization is transferred to the water protons during the second 2 ms CP period by either direct intermolecular dipolar contact (Chevelkov et al. 2005), exchange relayed transfer, or NOE (Lesage et al. 2008; Paulson et al. 2003). The fact that no cross-peaks originating from chemical exchange are detected is consistent with previous observations made in the supercooled regime (Lesage et al. 2008) (temperatures between 0 and −20°C, for which the supernatant water is not frozen), which showed that the height of the cross-peaks due to chemical exchange decreases with decreasing temperatures. In that temperature range, however, negative ROE-like correlations of weak height could be observed, which are not detected here. This might be due simply to the overall lower height of the water resonance as a consequence of broadening.

Figure 6e shows a similar proton-detected 2D HETCOR experiment, in which a 25 ms longitudinal proton mixing period was added after the second CP step. We observe strong non-specific correlations at the water frequency, confirming the presence of polarization exchange mechanisms on this longer time scale between the microcrystalline protein and the crystal-water pool. These signals are consistent with what is expected from chemical exchange followed by intramolecular spin diffusion at the longer timescale of this experiment, but dipolar transfer between protein spins and water protons cannot be excluded as the source either.

Optimizing sample preparation

We mentioned above that water removal, either physically or by freezing, potentially enhances spectral quality by improving the quality factor of the probe and reducing the power deposition. Also, the space left after physical removal of supernatant water can be re-filled with more protein. This is either possible by re-filling the rotor after rotation (= centrifugation) in the NMR probe, or by directly using g values comparable to that encountered in an NMR probe to fill the rotor in a centrifuge. To this goal, we developed filling tools that can be used in ultracentrifuges. The filling tool is illustrated schematically in Fig. 7. An example comparing spectra from a rotor filled with a normal centrifuge and an ultracentrifuge is given in Supporting figure S5, together with technical details on the filling protocol used for this example.

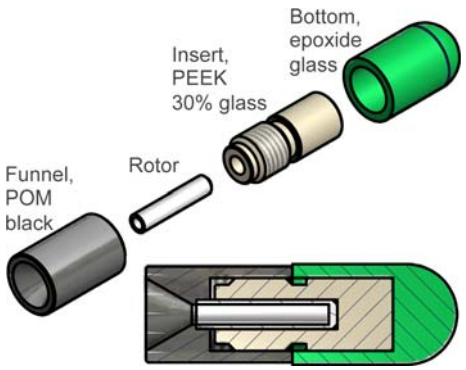

Fig. 7 Rotor filling tool for ultracentrifuge. The rotor is placed into an insert (here PEEK 30% glass), and a funnel is screwed directly onto the top of the MAS rotor, which is then inserted into the bottom part of the assembly. The tool shown here fits into the buckets of a swinging rotor (Beckman SW 40 Ti) and was tested up to speeds of 35,000 rpm (SW 40 Ti) corresponding to 210,000×*g* in a Beckman Optima™ L-90 K preparative ultracentrifuge. The tool shown fits a 3.2 mm Bruker rotor. Analogous devices were made for Bruker and Varian/Chemagnetics rotors ranging from 1.3 to 4 mm diameter. For rotors which have drive tips on the bottom, metal dummy drive tips were developed which can be placed on the bottom side of the rotor and, in contrast to the drive tips used for spectroscopy, can easily withstand the forces in the centrifuge

Conclusion

Two distinct water pools are observed in the proton NMR spectra of microcrystalline Crh, which differ significantly in spectroscopic properties including chemical shift, T_1 and T_2 relaxation and which are located in spatially different parts in the sample container. The two pools are identified as supernatant water, mainly located in the center of the rotor, and crystal water, located either inside the channels of each crystallite or directly surrounding them. The supernatant water and the crystal water do not exchange polarization on the timescale relevant for the NMR experiments ($\sim$1 s). The presence or absence of supernatant water has no influence on the state of the protein and it can thus be removed mechanically or by freezing (the crystal water remains mobile even at −30°C) to allow for proton detected NMR experiments carried out without water suppression schemes. Furthermore, the identification of the different pools explains experimental difficulties with water selection by T_2 filters in the past because the supernatant-water resonance was assumed to be identical to the crystal water. Managing the water magnetization of the crystal-water pool may lead to improved pulse schemes in solid-state NMR analogous to the development in solution NMR (Sklenár et al. 1993; Grzesiek and Bax 1993; Hiller et al. 2005). Such improvements are not limited to ^{1}H spectroscopy but apply to most solid-state NMR experiments on proteins. Removing the supernatant water from the sample allows for more protein to be added, significantly enhancing sensitivity, and also leading to better rf-performance for the NMR probe circuit.

Acknowledgement We thank Michel Juy for the picture of the Crh proteins arranged in the unit cell. This work was funded in part by CNRS, the French Research Ministry (ANR JCJC JC05_44957, ANR PCV 07 PROTEIN MOTION), the Swiss National Science Foundation (SNF) and the ETH Zurich.

References

Ader C, Schneider R, Seidel K, Etzkorn M, Becker S, Baldus M (2009) Structural rearrangements of membrane proteins probed by water-edited solid-state NMR spectroscopy. J Am Chem Soc 131:170–176

Aime S, Bruno E, Cabella C, Colombatto S, Digilio G, Mainero V (2005) HR-MAS of cells: a "Cellular Water Shift" due to water-protein interactions? Magn Res Med 54:1547–1552

Andronesi O, von Bergen M, Biernat J, Seidel K, Griesinger C, Mandelkow E, Baldus M (2008) Characterization of Alzheimer's-like paired helical filaments from the core domain of tau protein using solid-state NMR spectroscopy. J Am Chem Soc 130:5922–5928

Baldus M (2006) Solid-state NMR spectroscopy: molecular structure and organization at the atomic level. Angew Chem Int Ed Engl 45:1186–1188

Böckmann A (2007) High-resolution solid-state MAS NMR of proteins—Crh as an example. Magn Reson Chem 45:S24–S31

Böckmann A, Lange A, Galinier A, Luca S, Giraud N, Juy M, Heise H, Montserret R, Penin F, Baldus M (2003) Solid-state NMR sequential resonance assignments and conformational analysis of the 2 × 10.4 kDa dimeric form of the Bacillus subtilis protein Crh. J Biomol NMR 27(32):3–339

Böckmann A, Juy M, Bettler E, Emsley L, Galinier A, Penin F, Lesage A (2005) Water-protein hydrogen exchange in the microcrystalline protein Crh as observed by solid state NMR spectroscopy. J Biomol NMR 32:195–207

Castellani F, van Rossum B, Diehl A, Schubert M, Rehbein K, Oschkinat H (2002) Structure of a protein determined by solid-state magic-angle-spinning NMR spectroscopy. Nature 420:98–102

Cavanagh J, Fairbrother WJ, Palmer AG III, Skelton NJ (1996) Protein NMR spectroscopy: principles and practice. Elsevier Science, USA

Chevelkov V, Faelber K, Diehl A, Heinemann U, Oschkinat H, Reif B (2005) Detection of dynamic water molecules in a microcrystalline sample of the SH3 domain of alpha-spectrin by MAS solid-state NMR. J Biomol NMR 31:295–310

Chevelkov V, Faelber K, Schrey A, Rehbein K, Diehl A, Reif B (2007) Differential line broadening in MAS solid-state NMR due to dynamic interference. J Am Chem Soc 129:10195–10200

Chevelkov V, Diehl A, Reif B (2008) Measurement of 15 N–T1 relaxation rates in a perdeuterated protein by magic angle spinning solid-state nuclear magnetic resonance spectroscopy. J Chem Phys 128:052316

Etzkorn M, Martell S, Andronesi O, Seidel K, Engelhard M, Baldus M (2007) Secondary structure, dynamics, and topology of a seven-helix receptor in native membranes, studied by solid-state NMR spectroscopy. Angew Chem Int Ed Engl 46:459–462

Galinier A, Haiech J, Kilhoffer MC, Jaquinod M, Stulke J, Deutscher J, Martin-Verstraete I (1997) The *Bacillus subtilis* crh gene encodes a Hpr-like protein involved in carbon catabolite repression. Proc Natl Acad Sci USA 94:8439–8444

Giraud N, Blackledge M, Goldman M, Böckmann A, Lesage A, Penin F, Emsley L (2005) Quantitative analysis of backbone dynamics in a crystalline protein from Nitrogen-15 spin-lattice relaxation. J Am Chem Soc 127:18190–18201

Gottlieb HE, Kotlyar V, Nudelman A (1997) NMR chemical shifts of common laboratory solvents as trace impurities. J Org Chem 62:7512–7515

Grzesiek S, Bax A (1993) The importance of not saturating H2O in protein NMR: application to sensitivity enhancement and NOE measurements. J Am Chem Soc 115:12593–12594

Halle B (2003) Cross-relaxation between macromolecular and solvent spins: the role of long-range dipole couplings. J Chem Phys 119:12372–12385

Harbison GS, Roberts JE, Herzfeld J, Griffin RG (1988) Solid-state NMR detection of proton exchange between the bacteriorhodopsin Schiff base and bulk water. J Am Chem Soc 110:7221–7223

Hiller S, Wider G, Etezady-Esfarjani T, Horst R, Wüthrich K (2005) Managing the solvent water polarization to obtain improved NMR spectra of large molecular structures. J Biomol NMR 32:61–70

Hologne M, Faelber K, Diehl A, Reif B (2005) Characterization of dynamics of perdeuterated proteins by MAS solid-state NMR. J Am Chem Soc 127:11208–11209

Iwata K, Fujiwara T, Matsuki Y, Akutsu H, Takahashi S, Naiki H, Goto Y (2006) 3D structure of amyloid protofilaments of beta2-microglobulin fragment probed by solid-state NMR. Proc Natl Acad Sci U S A 103:18119–18124

Jaroniec CP, MacPhee CE, Bajaj VS, McMahon MT, Dobson CM, Griffin RG (2004) High-resolution molecular structure of a peptide in an amyloid fibril determined by magic angle spinning NMR spectroscopy. Proc Natl Acad Sci U S A 101:711–716

Jeener J, Meier BH, Bachmann P, Ernst RR (1979) Investigation of exchange processes by two-dimensional NMR spectroscopy. J Chem Phys 71:4546–4553

Juy M, Penin F, Favier A, Galinier A, Montserret R, Haser R, Deutscher J, Böckmann A (2003) Dimerization of Crh by reversible 3D domain swapping induces structural adjustments to its monomeric homologue HPr. J Mol Biol 332:767–776

Kumashiro KK, Schmidt-Rohr K, Thompson LK (1998) A novel tool for probing membrane protein structure: solid-state NMR with proton spin diffusion and X-nucleus detection. J Am Chem Soc 120:5043

Lange A, Becker S, Seidel K, Giller K, Pongs O, Baldus M (2005) A concept for rapid protein-structure determination by solid-state NMR spectroscopy. Angew Chem Int Ed Engl 44:2–5

Lesage A, Böckmann A (2003) Water–protein interactions in microcrystalline Crh measured by 1H–13C solid-state NMR spectroscopy. J Am Chem Soc 125:13336–13337

Lesage A, Emsley L, Penin F, Böckmann A (2006) Investigation of dipolar-mediated water-protein interactions in microcrystalline Crh by solid-state NMR spectroscopy. J Am Chem Soc 128:8246–8255

Lesage A, Gardiennet C, Loquet A, Verel R, Pintacuda G, Emsley L, Meier BH, Böckmann A (2008) Polarization transfer over the water–protein interface in solid proteins. Angew Chem Int Ed Engl 47:5851–5854

Loquet A, Bardiaux B, Gardiennet C, Blanchet C, Baldus M, Nilges M, Malliavin T, Bockmann A (2008) 3D structure determination of the Crh protein from highly ambiguous solid-state NMR restraints. J Am Chem Soc 130:3579–3589

Lorieau JL, McDermott AE (2006) Conformational flexibility of a microcrystalline globular protein: order parameters by solid-state NMR spectroscopy. J Am Chem Soc 128:11505–11512

Lorieau JL, Day LA, McDermott AE (2008) Conformational dynamics of an intact virus: order parameters for the coat protein of Pf1 bacteriophage. Proc Natl Acad Sci U S A 105:10366–10371

Mallamace F, Corsaro C, Broccio M, Branca C, Gonzalez-Segredo N, Spooren J, Chen SH, Stanley HE (2008) NMR evidence of a sharp change in a measure of local order in deeply supercooled confined water. Proc Natl Acad Sci U S A 105:12725–12729

Manolikas T, Herrmann T, Meier BH (2008) Protein structure determination from 13C spin-diffusion solid-state NMR. J Am Chem Soc 130:3959–3966

McDermott AE (2004) Structural and dynamic studies of proteins by solid-state NMR spectroscopy: rapid movement forward. Curr Opin Struct Biol 14:554–561

Meier BH, Ernst RR (1979) Elucidation of chemical exchange networks by two-dimensional NMR spectroscopy: the heptamethylbenzenonium ion. J Am Chem Soc 101:6441–6442

Modig K, Liepinsh E, Otting G, Halle B (2004) Dynamics of protein and peptide hydration. J Am Chem Soc 126:102–114

Otting G (1997) NMR studies of water bound to biological molecules. Prog NMR Spectrosc 31:259–285

Paulson EK, Morcombe CR, Gaponenko V, Dancheck B, Byrd RA, Zilm KW (2003) High-sensitivity observation of dipolar exchange and NOEs between exchangeable protons in proteins by 3D solid-state NMR spectroscopy. J Am Chem Soc 125:14222–14223

Ravindranathan KP, Gallicchio E, McDermott AE, Levy RM (2007) Conformational dynamics of substrate in the active site of cytochrome P450 BM-3/NPG complex: insights from NMR order parameters. J Am Chem Soc 129:474–475

Schneider R, Ader C, Lange A, Giller K, Hornig S, Pongs O, Becker S, Baldus M (2008) Solid-state NMR spectroscopy applied to a chimeric potassium channel in lipid bilayers. J Am Chem Soc 130:7427–7435

Segawa T, Kateb F, Duma L, Bodenhausen G, Pelupessy P (2008) Exchange Rate constants of invisible protons in proteins determined by NMR spectroscopy. Chembiochem 9:537–542

Skalicky JJ, Sukumaran DK, Mills JL, Szyperski T (2000) Toward structural biology in supercooled water. J Am Chem Soc 122:3230–3231

Skalicky JJ, Mills JL, Sharma S, Szyperski T (2001) Aromatic ring-flipping in supercooled water: implications for NMR-based structural biology of proteins. J Am Chem Soc 123:388–397

Sklenár V, Piotto M, Leppik R, Saudek V (1993) Gradient-tailored water suppression for 1H–15 N HSQC experiments optimized to retain full sensitivity. J Magn Reson A 102:241–245

Tycko R (2004) Progress towards a molecular-level structural understanding of amyloid fibrils. Curr Opin Struct Biol 14:96–103

Wasmer C, Lange A, Melckebeke HV, Siemer AB, Riek R, Meier BH (2008) Amyloid fibrils of the HET-s(218–289) prion form a beta solenoid with a triangular hydrophobic core. Science 319:1523

Zhou DH, Rienstra CM (2008) High-performance solvent suppression for proton detected solid-state NMR. J Magn Reson 192:167–172

Zhou DH, Shah G, Cormos M, Mullen C, Sandoz D, Rienstra CM (2007a) Proton-detected solid-state NMR spectroscopy of fully protonated proteins at 40 kHz magic-angle spinning. J Am Chem Soc 129:11791–11801

Zhou DH, Shea JJ, Nieuwkoop AJ, Franks WT, Wylie BJ, Mullen C, Sandoz D, Rienstra CM (2007b) Solid-state protein-structure determination with proton-detected triple-resonance 3D magic-angle-spinning NMR spectroscopy. Angew Chem Int Ed Engl 46:8380–8383